Theoretical investigation into the possibility of multiorbital magnetically ordered states in isotropically superstrained graphene

L. Craco
Instituto de Física, Universidade Federal de Mato Grosso, 78060-900, Cuiabá, MT, Brazil
(Received 10 May 2017; revised manuscript received 8 August 2017; published 6 October 2017)

Using density functional dynamical mean-field theory (DFDMFT) we address the problem of antiferromagnetic spin ordering in isotropically superstrained graphene. It is shown that the interplay between strain-induced one-particle band narrowing and sizable on-site electron-electron interactions naturally stabilizes a magnetic phase with orbital-selective spin-polarized p-band electronic states. While an antiferromagnetic phase with strong local moments arises in the p_z orbitals, the $p_{x,y}$ bands reveal a metallic state with quenched sublattice magnetization. We next investigate the possibility of superconductivity to emerge in this selective magnetoelectronic state. Our theory is expected to be an important step to understanding the next generation of flexible electronics made of Mott localized carbon-based materials as well as the ability of superstrained graphene to host coexisting superconductivity and magnetism at low temperatures.

DOI: 10.1103/PhysRevB.96.165412

I. INTRODUCTION

Natural graphene is a two-dimensional electronic system of carbon atoms arranged in a honeycomb lattice structure [1], with low energy electronic excitations described by linear dispersing, massless Dirac fermions. In recent years, graphene is attracting the attention of the wider scientific community due to its remarkable physical properties, suggesting its application in fields as diverse as photonics, sensor technology, and spintronics [2]. More precisely, graphene and its derivatives are expected to form the next generation of (radio frequency) transistors [3], flexible electronics [4,5], spintronics [6], and nanoelectronic devices [7]. However, the semimetallic nature of graphene with a Dirac like spectrum near the Fermi energy (E_F) seems to prevent its application as the host material for the next generation of flexible electronic devices [5] and stretchable transparent electrodes [4]. Monolayer and few layers graphene might also be useful as nanoscale superconducting devices, including superconducting single-photon detectors and nanoscale superconducting transistors [8], but the vanishing density of state (DOS) at E_F seems to prevent emergence of superconductivity in pristine graphene. On the other hand, due to its linear spectrum doped graphene has finite DOS near E_F where spin-fluctuation [9] or phonon [10] mediated superconductivity is expected to arise: Extant studies on doped graphene report superconducting transition temperatures (T_c) between 4 and 6 K and an usual normal state characterized by saturated resistivity below 40 K [11,12] followed by a linear-in-T dependence up to room temperatures [11]. Thus, to explore different routes towards bandstructure engineering and intrinsic magnetic phase fluctuations in graphene-based systems are problems of considerable importance. It should be noted here that a previous theoretical study on superconducting phases of pure and doped graphene (Ref. [13]) have raised the question of whether it would be possible to structurally modify graphene, so that this two-dimensional honeycomb lattice system would become magnetic or intrinsic superconducting. In the present study we hope to shed light on the important role of electronic interactions in superstrained graphene, providing a route to orbital-selective antiferromagnetism in strained p-band systems. Additionally, we investigate the possibility of s-wave superconductivity [13] to emerge in a selective magnetoelectronic state.

We remark that due to its extraordinary mechanical strength and flexibility [14], the potential to tune novel physical properties in strained graphene, including band-gap opening [15,16], global antiferromagnetism [17], metal-insulator transitions [18], and strain-enhanced superconductivity [19] as well as superconducting proximity effect in graphene under inhomogeneous strain [20] have been explored in recent years. Theoretically, at one-particle level strain can turn semimetal graphene metallic [21,22] and superconducting upon Li doping [19]. Experimentally, graphene can be stretched to 30% [4], however it is worth mentioning that carbon nanotube films with a serpentine morphology can be stretched one time 170% before failure [23], meaning that pristine graphene might have higher sheer elasticity and stretchability hitherto probed yet. In fact, experiments performed on graphene/poly(dimethyl siloxane) composites [24] seem to corroborate this suggestion by showing that these flexible conductors can support strains higher than 50% before they start to break. Thus, motivated by this and other studies on stretchable patterned graphene systems [25] as well as by an experimental study [14] establishing graphene as the strongest material ever seen in nature, in an earlier work [15] we carried out first-principles generalized gradient approximation plus dynamical mean-field theory (GGA+DMFT) [26] calculations to investigate changes in the electronic properties of isotropically superstrained graphene. It was shown in Ref. [15] that incorporation of on-site Coulomb correlations via GGA+DMFT an energy gap naturally opens up in superstrained graphene. We thus suggested that under extreme strain conditions the interplay between electron-electron interactions [27] and lattice strain would naturally induce Mott localization, i.e., the formation of a gapped excitation spectrum at low energies in stretchable graphene [15]. In this paper we extend this aspect and investigate the possibility of spin ordering and intrinsic multiorbital (MO) superconductivity in two-dimensional superstrained graphene.

It is now recognized that the competition between electron-electron interactions and band-itinerance drives the system towards a Mott metal-insulator transition point [28], which is

a manifestation of dynamical many-body effects in correlated electrons [29]. Historically, the Mott transition was considered to occur as a function of the expansion of the lattice constant L. In Mott's picture [30], a first-order transition from an insulator to a metallic state takes place at a critical value $L = L_c$. For $L > L_c$ a crystalline array of one-electron atoms should be in a charge insulating state whereas for $L < L_c$, one should have a metal. The charge gap at the Mott transition jumps discontinuously from a finite value to zero. Mott's original idea was to tune the U/W ratio between the on-site Coulomb repulsion U and the bare one-particle bandwidth W, or the kinetic energy of the free electron gas. This ratio, which defines the phase boundary between metallic and the Mott-insulating phases, holds true for narrow band systems in general [28]. However, the possibility of finding Mott metal-insulator instabilities in carbon-based materials [31] remains an open problem, since the naive expectation dictates that the itinerance (kinetic energy of p carriers) is appreciable compared to the electron-electron interactions, as distinct from d, f-band systems, where the electrons reside in narrower bands (hence the effective U/W is usually sizable). Thus, searching for and characterizing correlated electron physics in systems with active p bands is a problem of fundamental importance. With this caveat in mind, in our earlier works we have derived the correlated electronic structure of strained graphene [15,32], showing how it can be reshaped by electron-electron interaction effects. Particularly, in Ref. [32] we analyzed the MO electronic reconstruction associated with the interplay between U and W at currently acceptable strain conditions [4], revealing good theory-experiment agreement between scanning tunneling microscopy measurements on graphene nanobubbles and DFDMFT results for $U = 9.5$ eV and $L = 0.3209$ nm. (Noteworthy, the lattice constant of natural graphene is $L = 0.24669$ nm.) Additionally, based on GGA+DMFT calculations in Ref. [15] we have shown that Mott localization can be induced in superstrained graphene, $L = 0.3759$ nm. In this paper we extend our GGA+DMFT study and focus on the problem of correlation-induced localized moments and unconversional superconductivity in the ordered state of superstrained graphene system.

II. THEORY AND DISCUSSION

Before delving into the effect of dynamical electron-electron interactions in Fig. 1 we show the GGA spectral function of superstrained graphene [33]. At normal conditions, the sp^2 hybridization of atomic $s - p_{x,y}$ orbitals of carbon atoms in graphene and graphite create lateral σ bonds, and the remaining p_z orbital perpendicular to the plane form the nonhybridized π bands. As seen in Fig. 1 this scenario holds true for the p_z orbital channel, whose electronic DOS vanishes linearly at energies 0.658 eV above the Fermi energy E_F ($\omega = 0$). However, an overall reduction of the one-electron bandwidth W compared to natural graphene, including the energy position of the van-Hove singularities at the border of the Dirac dispersion, is found in the p_z band for the lattice constants varying from 0.24669 to 0.3759 nm [21]. Also interesting is the band electronic reconstruction within the planar $p_{x,y}$ orbitals, where the charge gap of natural graphene shrinks with increasing the lattice constant until it

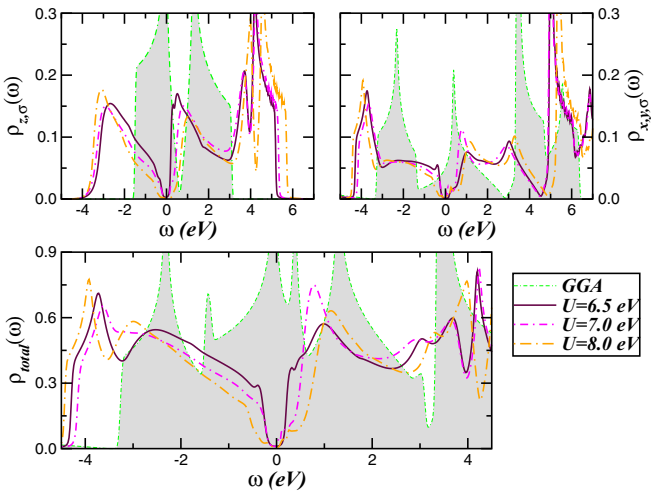

FIG. 1. GGA and GGA+DMFT orbital-resolved and total density of states (DOS) of paramagnetic superstrained graphene. Notice the electronic reconstruction on different orbitals induced by multiorbital electron-electron interactions. Compared to GGA DOS a relevant feature to see is the Mott localization at low energies in all active p bands.

is fully suppressed at large L [21], as shown in Fig. 1 for $L = 0.3759$ nm. Thus, the central result to be seen in the GGA DOS is the orbital-selective (OS) p-band metallicity and the one-particle band narrowing, which can be tuned by pulling the carbon atoms further apart in accordance with Mott ideas. These are the crucial ingredients in determining the excitation spectrum and the ground state properties of superstrained graphene.

The on-site Coulomb interaction parameter for natural graphene is $U = 9.3$ eV. [27] Owing to the metallic p-band DOS in superstrained graphene with $L = 0.3759$ nm, one expects the Hubbard U (or the on-site Coulomb interaction) to be partially screened as in natural graphene, where high energy excitations involving the σ bands are considered to screen short-ranged Hubbard-like interactions in this and related carbon allotropes [34]. Thus, in our study we choose renormalized U values to reveal an antiferromagnetic electronic state in superstrained graphene. The many-body Hamiltonian relevant for strained graphene [15,32] is $H = H_0 + H_{\rm int}$ with $H_0 = \sum_{\mathbf{k}a\sigma} \epsilon_a(\mathbf{k}) c^\dagger_{\mathbf{k}a\sigma} c_{\mathbf{k}a\sigma}$, and

$$H_{\rm int} = U \sum_{ia} n_{ia\uparrow} n_{ia\downarrow} + \sum_{ia\neq b} U' n_{ia} n_{ib} - J_H \sum_{ia\neq b} \mathbf{S}_{ia} \cdot \mathbf{S}_{ib} \,. \tag{1}$$

Here, $a = x, y, z$ label the diagonalized p bands and $\epsilon_a(\mathbf{k})$ is the one-electron band dispersion, which encodes details of the one-electron (GGA) band structure. $U' \equiv U - 2J_H$, with U, U' being the intra- and interorbital Coulomb repulsion and J_H is Hund's rule coupling. Effect of tuning the one-band dispersions are read off from $\epsilon_a(\mathbf{k})$: These are inputs for MO DMFT which generate a Mott insulating state for $L = 0.3759$ nm, as shown below. We use MO DMFT for the three-orbital model of strained graphene with the MO iterated-perturbation theory (MO-IPT) as impurity solver. The detailed formulation of MO-IPT for correlated electron systems has

already been developed [35] (similar interpolative ansatz for MO systems can be found in Ref. [36]) and used in the context of layered carbon-based systems [15,32,37], so we do not repeat the equations here.

A. Paramagnetic state

Since the dependence of electron-electron interactions in the excitation spectrum graphene-based systems is quite subtle and not yet fully understood [38], in Fig. 1 we display the excitation spectrum that emerges from dynamical MO electron-electron interactions in paramagnetic superstrained graphene for $L = 0.3759$ nm. The formation of the Mott-Hubbard insulating band gap at low energies with concomitant appearance of lower- (LHB) and upper-Hubbard (UHB) bands on different orbitals at high energies is visible in the GGA+DMFT results for three different values of U and fixed $J_H = 0.4$ eV. (Our choice for J_H is in accordance with values estimated within GGA on a different local moment problem in graphene [39].) As seen electron-electron interactions strongly modify the bare, GGA spectral functions. MO dynamical correlations arising from U, U' and J_H lead to spectral weight redistribution over large energy scales and the formation of LHB and UHB at high energies and a narrow Mott gap near E_F for all orbitals. Noticeable differences in the spectral weight transfer (SWT) are seen between the p_z and $p_{x,y}$ channels. Within the p_z orbital the LHB at $\omega \approx 2.9$ eV for $U = 7.0$ eV is clearly resolved. SWT is also seen within the planar orbitals. In these channels the electronic states within the antibonding band in GGA partly transfer to higher energies but the spectral lineshape above 5.0 eV is close to that found in GGA.

B. Antiferromagnetic state

Similar to Ref. [15] our analysis above was restricted to the paramagnetic phase. However, this phase is not expected to be stable at very low temperatures in the limit of strong Coulomb interaction even for honeycomb lattices with arbitrary interaction strength [40], including strained graphene [17]. It is well known that in the large U limit the one-band Hubbard model reduces to the antiferromagnetic Heisenberg model [41], with an effective exchange interaction $J = t^2/U$ (t is the nearest-neighbor hopping amplitude). An instability of the paramagnetic state against the formation of a spin-density wave is also expected in honeycomb lattice systems with sizable to strong Coulomb interaction parameters [40]. In the antiferromagnetic phase the period of the unit cell of the lattice is doubled due to the reduced translational symmetry. Consequently, the volume of the magnetic Brillouin zone is reduced to one half of the volume in the paramagnetic state [42]. These changes in the symmetries of the system can be taken into account by introduction of an AB-sublattice structure and reformulating the theory for the paramagnetic state on an enlarged unit cell containing two sublattices, A and B. Therefore, in the search for an ordered phase in superstrained graphene one needs to extend the bipartite Green's function formalism for the one- and three-band Hubbard models [42,43] to the MO case relevant to antiferromagnetically ordered graphenelike systems. In this regime the retarded, one-particle Green's function at site A or B (A/B), orbital a, and spin σ

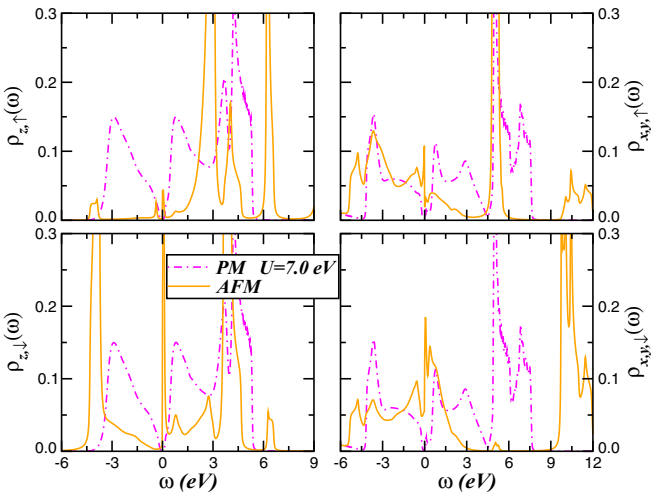

FIG. 2. GGA+DMFT ($U = 7.0$ eV) orbital- and spin-resolved DOS of paramagnetic (PM) and antiferromagnetic (AFM) superstrained graphene. Notice the electronic reconstruction on different orbitals across the magnetic transition and the appearance of an orbital-selective insulating-metallic state in the antiferromagnetically ordered state of superstrained graphene.

reads

$$G^{A/B}_{a\sigma} = \int_{-\infty}^{\infty} d\varepsilon \rho^{o}_{a}(\varepsilon) \frac{\xi^{B/A}_{a\sigma}(\omega)}{\xi^{A}_{a\sigma}(\omega)\xi^{B}_{a\sigma}(\omega) - \varepsilon^2} \,. \qquad (2)$$

Here $\xi^{A/B}_{a\sigma}(\omega) = \omega + \mu - \Sigma^{A/B}_{a\sigma}(\omega)$, with $\rho^{0}_{a}(\varepsilon)$ and $\Sigma_a(\omega)$ being, respectively, the GGA DOS and the self energy of orbital a, and μ the chemical potential of the system. For the sake of simplicity, in the antiferromagnetic state it is sufficient to perform the calculations for the A sublattice due to the additional symmetry $G^{A}_{a\sigma} = G^{B}_{a\bar{\sigma}}$ of the bipartite lattice [42].

Let us now present our results for the Néel ordered state [17] of superstrained graphene. In the following we concentrate on the one-particle MO spectrum of the A sublattice [$\rho_{a,\sigma}(\omega) \equiv -\frac{1}{\pi} Im G^{A}_{a\sigma}(\omega)$]. As seen in Fig. 2, when the system enters the antiferromagnetic phase the spectral functions of up and down spin for the p bands become inequivalent, yielding a finite sublattice magnetization, $m = \Sigma_a |\langle n_{a\uparrow}\rangle - \langle n_{a\downarrow}\rangle|$. An important effect is the overall SWT in p_z channel and, as expected, the formation of strong local moment (LHB) in $\rho_{z\downarrow}$ DOS. (From symmetry reasons the spin-$\uparrow$ electron occupy the B sublattice.) Surprisingly, on the other hand, is the appearance of a metallic electronic state with reduced spin polarization in the planar bands, which shows pseudogap features at energies near E_F. Based on our results in Fig. 2 we thus predict that strong orbital reconstruction would be seen in crossing the paramagnetic to the long-range ordered phase of superstrained graphane. Additionally in Fig. 3 we compare our GGA+DMFT results for two values of the on-site Coulomb interact U. With increasing U towards its realistic value [27] (i.e., $U \approx 9.0$ eV) full electronic polarization is found in the p_z ordered state, with the LHB being transferred to high binding energies. Notwithstanding, due to small $U/W \approx 1$ ratio and strong electronic reconstruction the Néel state in the planar orbitals is rather weakly ordered and full spin

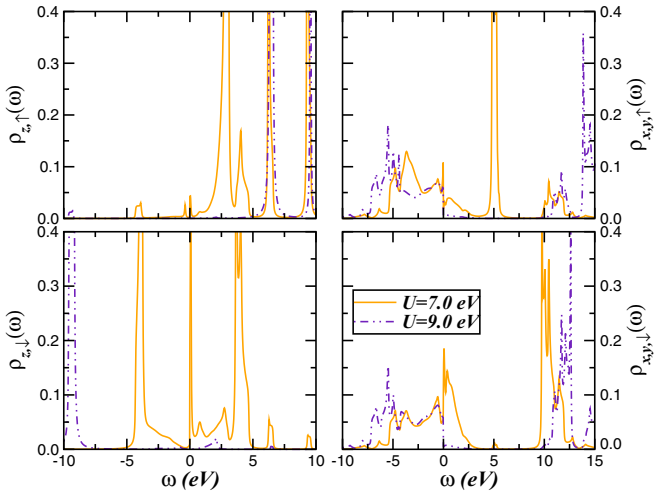

FIG. 3. Effect of electron-electron interactions on the GGA+DMFT orbital- and spin-resolved DOS of antiferromagnetic superstrained graphene. Notice the large transfer of spectral weight and the formation of localized moments in the p_z channels as well as the electronic reconstruction on the planar (x,y) bands at low energies. Particularly relevant feature to be seen is the electron localization induced on all orbital states for $U = 9.0$ eV.

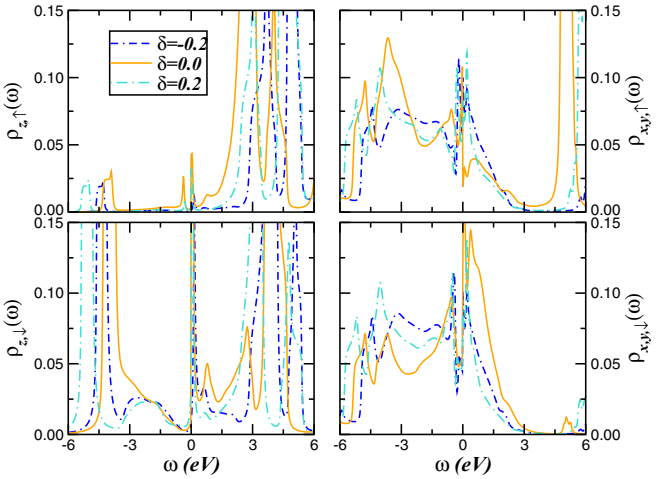

FIG. 4. Effect of electron/hole doping in the orbital- and spin-resolved GGA+DMFT ($U = 7.0$ eV) DOS for the antiferromagnetically ordered state of superstrained graphene. Notice the narrow quasiparticle resonances at the spin-resolved p_z bands and the downshift of valence band states with increasing the electron concentration.

polarization is expected to be seen only at higher U values. However, the position of LHB and UHB in the spectra are clearly shifted in energy with respect to each other as expected for itinerant systems approaching magnetic phase instabilities. Taken together, the changes in SWT in Figs. 2 and 3 can be ascribed to an internal molecular field, generated by the finite sublattice magnetization [42] on different orbital channels. Importantly, our result in Fig. 3 implies that the charge carriers in the antiferromagnetically ordered state of superstrained graphene have a dual nature, where effectively localized p_z states coexist with incoherent $p_{x,y}$ electronic excitations at $7.0 < U < 9.0$ eV. Such incoherent behavior results from scattering between effectively spin-localized and quasi-itinerant electron components of the full DMFT matrix propagators.

To gain insights on the interplay between electron-electron interactions and (electron/hole) doping on the multiple structure of the antiferromagnetically ordered state of superstrained graphene, in Fig. 4 we display our GGA+DMFT for $U = 7.0$ eV and $J_H = 0.4$ eV. Large SWT is visible upon addition/removal of charge carries in antiferromagnetic superstrained graphene. Particularly interesting is the narrow Kondo-like quasiparticle resonance in the majority p_z which crosses E_F with increasing the electron concentration, $\delta = 0.2$. This in turn induces half-metallicity in the out-of-plane orbital channel. Thus, similar to $CePt_3P$ low-temperature superconductor [44], our results suggest a coexistence of antiferromagnetic ordering and U'-induced orbital Kondo effect [45] in superstrained graphene. Moreover, the tiny pseudogap observed in the $p_{x,y\uparrow}$ electronic states gives away to quasiparticle resonances at low energies. However, as can be seen in Fig. 4 (lower-right panel), our self-consistent GGA+DMFT calculation also resolves a pseudogap feature near E_F in $p_{x,y\downarrow}$ electronic channel. This behavior is expected to MO metallic systems close to electronic localization, where strong orbital and spin fluctuations prevent the Fermi liquid fixed point. In our superstrained graphene system the transfer of spectral weight found in this strange metallic phase can be traced to a dynamical scattering process that leads to electron mass enhancement, which is not expected for massless Dirac fermion systems like natural graphene [46]. Our work calls for low-temperature electrical transport studies in superstrained graphene. These studies will constitute a proof to selective electronic delocalization and nonglobal electron-frozen antiferromagnetism as well as the importance of treating dynamical correlations adequately to reveal a variety of unexplored responses in complex materials under extreme strain conditions.

C. Superconducting state in a selective antiferromagnetic metal

To better understand the selective MO physics of superstrained graphene, it can be a useful and, at the same time, an interesting exercise to investigate the changes of low energy electronic states across the normal-to-superconducting phase transition. However, in view of the complexity of the problem [47], we only restrict ourselves to a qualitative discussion. Since Fermi liquid quasiparticles are not stable excitations in the strange metal coexisting with an antiferromagnetic background, instabilities to ordered states via (particle-particle) BCS-like pairing of well defined Fermi liquid quasiparticles are untenable. In strange metals, the coherent one-electron hopping term is irrelevant in a renormalization group sense [48]. Hence, superconducting ordered states may arise via coherent two-particle hopping, which becomes more relevant when the one-electron hopping term is irrelevant: The situation is analogous to coupled Luttinger liquids [49] as discussed in an earlier study of multiband superconductivity in iron-based superconductors [50]. Given the selective incoherent metallic state within DMFT in our case, the above analogy tells

us that residual, intersite, and interorbital (in MO systems) two-particle interactions can generate ordered states directly from the strange metal.

Following the philosophy used earlier [51] for pressurized solid O_2 p-band superconductor we restrict ourselves to the x,y orbital sector, where the interaction in the Cooper channel reads $H_{\rm pair} = \frac{1}{2}\sum_{a,b,k,k'} V_{ab}(k,k')c^{\dagger}_{a,k,\uparrow}c^{\dagger}_{b,-k,\downarrow}c_{b,-k',\downarrow}c_{a,k',\uparrow}$. Here $a,b = x,y$ and the scattering vertex is $V_{ab}(k,k',\omega) = g^2\chi_{ab}(k-k',\omega)$ with $\chi_{ab}(k-k',\omega)$ being the interorbital susceptibility. Decoupling $H_{\rm pair}$ in the particle-particle channel using Gorkov's formalism [52] gives $H^{MF}_{\rm pair} = \sum_{abk}[\Delta_{ab}(k)(c^{\dagger}_{ka\uparrow}c^{\dagger}_{-kb\downarrow} + \text{H.c.})]$, where $\Delta_{ab}(k) = \frac{1}{2}V_{ab}\langle c_{-kb\downarrow}c_{ka\uparrow}\rangle$. This represents an interorbital pairing instability of the strange metal state near the superconducting transition in superstrained graphene. Albeit different pairing symmetries have been proposed for graphenelike systems [13,53,54], a plausible assumption to be made here is that the superconducting gap function is momentum independent, i.e., $\Delta_{ab}(k) \equiv \Delta$, for the (multiband) s-wave [13,54] case of superconducting graphene. Thus, aiming to shine light on the changes in the excitation spectrum of superstrained graphene across the superconducting phase transition we have extended the normal state electronic structure calculation to treat $H_{\rm pair}$ above within GGA+DMFT formalism for the superconducting state. Using our assumption for the s-wave superconducting gap function Δ the GGA+DMFT equations for the bipartite lattice are readily extendable to the superconducting regime. As in the case of superconductivity arising from an instability of a correlated paramagnetic state [50,55], the matrix one-particle Green's function ($\mathbf{G}_{ab}$) has normal and anomalous components yielding renormalized $G_{aa}(\equiv G_a)$ propagators, which are solved by extending the antiferromagnetic normal state solution to include an explicit pair-field term. Including the pair field, the DMFT propagators of orbital a at site A can be written as

$$G^{A}_{a\sigma} = \int_{-\infty}^{\infty} d\varepsilon \rho^{o}_{a}(\varepsilon)\frac{1}{\xi^{A}_{a\sigma}(\omega) - \frac{\varepsilon^2}{\xi^{B}_{a\sigma}(\omega)} - \frac{\Delta^2}{\omega+\varepsilon+\Sigma^{*A}_{b\bar{\sigma}}(\omega)}}, \quad (3)$$

where the $*$ in $\Sigma^{*A}_{b\bar{\sigma}}(\omega)$ denotes complex conjugation [55].

We now describe our results within the superconducting state of superstrained graphene. Using the GGA+DMFT solutions for $U = 7.0$ eV, in Fig. 5 (left panels) we show the changes induced by superconductivity in the spin- and orbital-resolved spectral functions of superstrained graphene. As seen the minority $p_{x,y,\downarrow}$ channel is the most affected in the limit of strong s-wave pairing mechanism. Also visible is the emergence of a superconducting gap and sharp singularities at low energies across the superconducting instability. However, antiferromagnetic normal state localization in the p_z propagator $[G^{A}_{z\sigma}(\omega)]$ prevents opening up of a clean superconducting gap in the $p_{x,y}$ DOS at low energies, suggesting that superstrained graphene might be a promising candidate to be added to the antiferromagnetic superconductors material class [56] which also display gapless band dispersions in their electronic spectrum.

Additionally, we shall notice here that the antiferromagnetically ordered state in the p_z channel is not suppressed by the superconducting instability (not shown), and this might be related to the fact that spin fluctuations are quenched in this

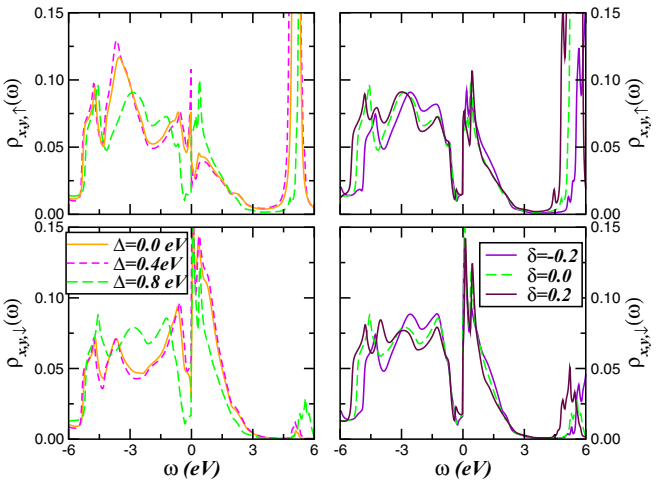

FIG. 5. Spin-resolved GGA+DMFT ($U = 7.0$ eV) DOS for pure (left panels) and doped (right panels) superstrained graphene. Left panels display the electronic reconstruction of the antiferromagnetic ($\Delta = 0.0$) phase towards a s-wave superconducting state. Right panels show the effect of electron/hole doping on the $p_{x,y}$-electronic states of superconducting ($\Delta = 0.8$ eV) superstrained graphene.

electronic channel and the fact that the excitation spectrum is already gapped in the correlated normal state. Remarkable as well is the fact that the pseudosuperconducting gap is strongly asymmetric and sets in mostly in the valence band states. As a key finding, we reveal a leading-edge asymmetry near E_F as observed in Li-decorated monolayer graphene [57], providing support to our unconventional superconducting state. Finally, weak SWT from low to high energies occurs in all p bands as seen in Fig. 5. This suggests an orbital selective coupling of the carrier propagators to overdamped charge and spin excitations which could be tested in future resonant inelastic x-ray scattering studies [58]. Future tunneling spectroscopy (dI/dV) measurements are also called for to corroborate our prediction of an anisotropic (in energy) profile and the small changes in the one-particle spectral function upon electron/hole doping (Fig. 5 right panels) of superconducting superstrained graphene.

III. CONCLUSION

In conclusion, we have performed GGA+DMFT calculations for a realistic multiorbital Hubbard model to explore the correlated nature of the excitation spectrum which emerges in the antiferromagnetically ordered state of superstrained graphene. In a regime of isotropically large lattice distances, the interplay between one-particle band narrowing and multiorbital electron-electron interactions pushes superstrained graphene into an orbital-selective electronic state characterized by coexisting localized moments and itinerant electronic states. Additionally, we have explored the possibility of antiferromagnetic and superconducting phase coexistence, showing that the two orders might be intimately connected as in $In_3Cu_2VO_9$ honeycomb lattice compound [59]. Our microscopic description of coupled multiorbital Hubbard

interactions is expected to be generally applicable to understanding antiferromagnetism in stretchable graphene [17] and the underlying electronic state of superconducting graphene networks [10–12].

ACKNOWLEDGMENTS

This work is supported by CNPq (Grant No. 307487/2014-8). Acknowledgment is also made to Theoretical Chemistry department at Technical University Dresden for hospitality.

[1] A. H. C. Neto, F. Guinea, N. M. R. Peres, K. S. Novoselov, and A. K. Geim, Rev. Mod. Phys. **81**, 109 (2009).
[2] D. R. Cooper, B. D'Anjou, N. Ghattamaneni, B. Harack, M. Hilke, A. Horth, N. Majlis, M. Massicotte, L. Vandsburger, E. Whiteway, and V. Yu, arXiv:1110.6557.
[3] Y. Wu, Y.-M. Lin, A. A. Bol, K. A. Jenkins, F. Xia, D. B. Farmer, Y. Zhu, and P. Avouris, Nature (London) **472**, 74 (2011); see also, Y.-M. Lin, C. Dimitrakopoulos, K. A. Jenkins, D. B. Farmer, H.-Y. Chiu, A. Grill, and P. Avouris, Science **327**, 662 (2010).
[4] K. S. Kim, Y. Zhao, H. Jang, S. Y. Lee, J. M. Kim, K. S. Kim, J.-H. Ahn, P. Kim, J.-Y. Choi, and B. H. Hong, Nature (London) **457**, 706 (2009).
[5] C. F. Guo, Q. Liu, G. Wang, Y. Wang, Z. Shi, Z. Suo, C.-W. Chu, and Z. Ren, PNAS **112**, 12332 (2015).
[6] D. Pesin and A. H. MacDonald, Nat. Mater. **11**, 409 (2012).
[7] J. Nilsson, A. H. C. Neto, F. Guinea, and N. M. R. Peres, Phys. Rev. B **76**, 165416 (2007).
[8] See, T. Morshedloo, M. R. Roknabadi, M. Behdani, M. Modarresi, and A. Kazempour, Comput. Mater. Sci. **124**, 183 (2016), and references therein.
[9] N. M. R. Peres, M. A. N. Araújo, and D. Bozi, Phys. Rev. B **70**, 195122 (2004).
[10] G. Profeta, M. Calandra, and F. Mauri, Nat. Phys. **8**, 131 (2012); M. Einenkel and K. B. Efetov, Phys. Rev. B **84**, 214508 (2011).
[11] J. Chapman, Y. Su, C. A. Howard, D. Kundys, A. N. Grigorenko, F. Guinea, A. K. Geim, I. V. Grigorieva, and R. R. Nair, Sci. Rep. **6**, 23254 (2016).
[12] S. Ichinokura, K. Sugawara, A. Takayama, T. Takahashi, and S. Hasegawa, ASC Nano **10**, 2761 (2016).
[13] B. Uchoa and A. H. C. Neto, Phys. Rev. Lett. **98**, 146801 (2007).
[14] C. Lee, X. Wei, J. W. Kysar, and J. Hone, Science **321**, 385 (2008).
[15] L. Craco, S. S. Carara, and S. Leoni, Phys. Rev. B **94**, 165168 (2016).
[16] Z. H. Ni, T. Yu, Y. H. Lu, Y. Y. Wang, Y. P. Feng, and Z. X. Shen, ACS Nano **2**, 2301 (2008).
[17] B. Roy, F. F. Assaad, and I. F. Herbut, Phys. Rev. X **4**, 021042 (2014).
[18] S. H. Lee, S. Kim, and K. Kim, Phys. Rev. B **86**, 155436 (2012); H. K. Tang, E. Laksono, J. N. B. Rodrigues, P. Sengupta, F. F. Assaad, and S. Adam, Phys. Rev. Lett. **115**, 186602 (2015).
[19] J. Pešić, R. Gajić, K. Hingerl, and M. Belić, Europhys. Lett. **108**, 67005 (2014).
[20] L. Covaci and F. M. Peeters, Phys. Rev. B **84**, 241401(R) (2011).
[21] G. Gui, J. Li, and J. Zhong, Phys. Rev. B **78**, 075435 (2008).
[22] M. Farjam and H. Rafii-Tabar, Phys. Rev. B **80**, 167401 (2009).
[23] D. J. Lipomi, M. Vosgueritchian, B. C.-K. Tee, S. L. Hellstrom, J. A. Lee, C. H. Fox, and Z. Bao, Nat. Nanotechnol. **6**, 788 (2011).
[24] Z. Chen, W. Ren, L. Gao, B. Liu, S. Pei, and H.-M. Cheng, Nat. Mater. **10**, 424 (2011).
[25] J. Yun, Y. Lim, G. N. Jang, D. Kim, S. J. Lee, H. Park, S. Y. Hong, G. Lee, G. Zi, and J. S. Ha, Nano Energy **19**, 401 (2016).
[26] G. Kotliar, S. Y. Savrasov, K. Haule, V. S. Oudovenko, O. Parcollet, and C. A. Marianetti, Rev. Mod. Phys. **78**, 865 (2006).
[27] T. O. Wehling, E. Şaşıoğlu, C. Friedrich, A. I. Lichtenstein, M. I. Katsnelson, and S. Blügel, Phys. Rev. Lett. **106**, 236805 (2011).
[28] M. Imada, A. Fujimori, and Y. Tokura, Rev. Mod. Phys. **70**, 1039 (1998).
[29] A. Georges, G. Kotliar, W. Krauth, and M. J. Rozenberg, Rev. Mod. Phys. **68**, 13 (1996).
[30] N. F. Mott, *Metal-Insulator Transitions* (Taylor and Francis, London, 1974).
[31] P. Durand, G. R. Darling, Y. Dubitsky, A. Zaopo, and M. J. Rosseinsky, Nat. Mater. **2**, 605 (2003).
[32] L. Craco, D. Selli, G. Seifert, and S. Leoni, Phys. Rev. B **91**, 205120 (2015).
[33] Details of the GGA calculation and relevant references on the GGA implementation can be found in Ref. [15].
[34] Y. Gan, G. A. de la Peña, A. Kogar, B. Uchoa, D. Casa, T. Gog, E. Fradkin, and P. Abbamonte, Phys. Rev. B **93**, 195150 (2016).
[35] M. S. Laad, L. Craco, and E. Müller-Hartmann, Phys. Rev. B **73**, 045109 (2006); L. Craco, *ibid.* **77**, 125122 (2008).
[36] P. Pou, R. Pérez, F. Flores, A. L. Yeyati, A. Martin-Rodero, J. M. Blanco, F. J. García-Vidal, and J. Ortega, Phys. Rev. B **62**, 4309 (2000); N. Dasari, W. R. Mondal, P. Zhang, J. Moreno, M. Jarrell, and N. S. Vidhyadhiraja, Eur. Phys. J. B **89**, 202 (2016).
[37] L. Craco, M. S. Laad, S. Leoni, and A. S. de Arruda, Phys. Rev. B **87**, 155109 (2013).
[38] V. N. Kotov, B. Uchoa, V. M. Pereira, F. Guinea, and A. H. C. Neto, Rev. Mod. Phys. **84**, 1067 (2012).
[39] M. Casartelli, S. Casolo, G. F. Tantardini, and R. Martinazzo, Phys. Rev. B **88**, 195424 (2013).
[40] L. M. Martelo, D. Dzierzawa, L. Siffert, and B. Baeriswyl, Z. Phys. B **103**, 335 (1997); S. Sorella and E. Tosatti, Europhys. Lett. **8**, 699 (1992).
[41] P. W. Anderson, in *Solid State Physics: Advances in Research and Applications*, edited by F. Seitz and D. Turnbull (Academic, New York, 1963), Vol. 14, p. 99.
[42] T. Maier, M. B. Zölfl, T. Pruschke, and J. Keller, Physica B (Amsterdam) **259-261**, 747 (1999).
[43] L. Craco and M. A. Gusmão, Phys. Rev. B **54**, 1629 (1996).
[44] J. Chen, Z. Wang, S. Zheng, C. Feng, J. Dai, and Z. Xub, Sci. Rep. **7**, 41853 (2017).

[45] L. Craco, M. S. Laad, and E. Müller-Hartmann, Phys. Rev. Lett. **90**, 237203 (2003).
[46] K. S. Novoselov, A. K. Geim, S. V. Morozov, D. Jiang, M. I. Katsnelson, I. V. Grigorieva, S. V. Dubonos, and A. A. Firsov, Nature (London) **438**, 197 (2005).
[47] See, for example, D. E. Almeida, R. M. Fernandes, and E. Miranda, Phys. Rev. B **96**, 014514 (2017), and references therein.
[48] P. W. Anderson, *The Theory of Superconductivity in the High-*T_c *Cuprates*, Princeton Series in Physics (Oxford University Press, Princeton, 1997).
[49] E. Giamarchi, *Quantum Physics in One Dimension* (Oxford University Press, Princeton, 2004).
[50] M. S. Laad and L. Craco, Phys. Rev. Lett. **103**, 017002 (2009).
[51] L. Craco, M. S. Laad, and S. Leoni, Sci. Rep. **7**, 2632 (2017).
[52] R. Fehrenbacher and M. R. Norman, Phys. Rev. Lett. **74**, 3884 (1995).
[53] F. M. D. Pellegrino, G. G. N. Angilella, and R. Pucci, Eur. Phys. J. B **76**, 469 (2010); J. Vučičević, M. O. Goerbig, and M. V. Milovanović, Phys. Rev. B. **86**, 214505 (2012).
[54] H.-Y. Lu, S. Chen, Y. Xu, L.-Q. Zhang, D. Wang, and W.-S. Wang, Phys. Rev. B **88**, 085416 (2013).
[55] A. Garg, H. R. Krishnamurthy, and M. Randeria, Phys. Rev. B **72**, 024517 (2005).
[56] A. I. Buzdin and L. N. Bulaevskii, Sov. Phys. Usp. **29**, 412 (1986).
[57] B. M. Ludbrook, G. Levy, P. Nigge, M. Zonno, M. Schneider, D. J. Dvorak, C. N. Veenstra, S. Zhdanovich, D. Wong, P. Dosanjh, C. Straßer, A. Stöhr, S. Forti, C. R. Ast, U. Starke, and A. Damascelli, PNAS **112**, 11795 (2015).
[58] C. Monney, T. Schmitt, C. E. Matt, J. Mesot, V. N. Strocov, O. J. Lipscombe, S. M. Hayden, and J. Chang, Phys. Rev. B **93**, 075103 (2016).
[59] Y. Zhong, L. Zhang, H.-T. Lu, and H.-G. Luo, Physica B (Amsterdam) **462**, 1 (2015).